Chiral Recognition in Self-complexes of Tetrahydroimidazo[4,5-*d*]imidazole Derivatives: From Dimers to Heptamers

Ibon Alkorta,* Oscar Picazo, and José Elguero

Instituto de Química Médica, Juan de la Cierva, 3, 28006-Madrid, Spain

Received: November 28, 2005

The chiral discrimination in the self-association of chiral 1,3a,4,6a-tetrahydroimidazo[4,5-*d*]imidazoles has been studied using density functional theory methods. Clusters from dimers to heptamers have been considered. The heterochiral dimers (*RR:SS* or *SS:RR*) are more stable than the homochiral ones (*RR:RR* or *SS:SS*) with energy differences up to 17.5 kJ/mol. Besides, in larger clusters the presence of two adjacent homochiral molecules impose an energetic penalty when compared to alternated chiral systems (*RR:SS:RR:SS*...). The differences in interaction energy within the dimers of the different derivatives have been analyzed based on the atomic energy partition carried out within the atoms in molecules framework. The mechanism of proton transfer in the homo- and heterochiral dimers shows large transition-state barriers except in those cases in which a third additional molecule is involved in the transfer. The optical rotatory power of several clusters of the parent compound have been calculated and rationalized based on the number of homochiral interactions and the number of monomers of each enantiomer within the complexes.

Introduction

The chiral discrimination, defined as the interaction energy difference for the two enantiomers of a given molecule acting on the same enantiomer of another,[1] is a process going back to Pasteur's experiment of spontaneous resolution of crystals of sodium ammonium tartrate.[2] The importance of chiral discrimination in biology and chemical reactivity is well known even though their mechanisms are not properly understood.

Several theoretical articles have addressed the problem of chiral self-recognition in hydrogen bonded complexes as in the case of a series of α-amino alcohols,[3] in complexes of compounds with axial chirality,[4] in dimers of pyrrolo[2,3-*c*]-pyrroles,[5] peptide models,[6] cysteine dimers,[7] phosphinic acid derivatives,[8] 1,8a-dihydro-1,8-naphthyridines,[9] cyclic α-hydroxy carbonyl compounds,[10] as well as in dimers and trimers of sulfoxide derivatives.[11] In addition, the corresponding proton-transfer processes have been examined for several of the systems previously mentioned. Moreover, the solvent effect on the chiral discrimination has been studied in dimers of hydrogen peroxide, hydrazine, and their methyl derivatives.[12,13] As well, the diastereomeric interaction between hydrogen peroxide, as chiral probe, and other chiral molecules such as oxirane[14] and lactic acid[15] has been analyzed. Finally, the interaction of 2-naphthyl-1-ethanol with chiral and nonchiral alcohols has been experimentally and theoretically studied.[16]

The properties of chiral clusters in the gas phase have been experimentally determined using different spectroscopic techniques.[17] Thus, King and Howard reported a microwave study of the heterochiral dimer of 2-butanol,[18] and Suhm et al. have examined the dimers of glycidol and clusters of methyl lactate derivatives by means of Fourier transform infrared (FTIR) spectroscopy.[19,20] As well, Beu and Buck found evidence of the presence of different chiral isomers in the IR spectra of hydrazine clusters,[21] and Zehnacker-Rentien et al. have studied the complexes of 2-naphthyl-1-ethanol with chiral systems using IR/UV double resonance spectroscopy.[22,23] It also should be mentioned that Speranza et al. used resonance-enhanced two-photon ionization (R2PI) spectroscopy to study the chiral complexes of alcohol dimers[24,25] and mass spectrometry in the case of metallic complexes of α-aminophosphonic acids.[26]

In the present article, the self-association of chiral 1,3a,4,6a-tetrahydroimidazo[4,5-*d*]imidazoles (Chart 1) from dimers up to heptamers has been studied by means of density functional theory (DFT) calculations. For the dimers, several substituents have been considered in positions 3a and 6a such as H, F, Cl, CH_3, CN, CCH, and CF_3. To be able to analyze the energy redistribution due to the complex formation and atomic contribution to the chiral discrimination, an atomic energy partition has been carried out using the electron density analysis with the atoms in molecules (AIM) methodology. In addition, the proton-transfer surface within the monomers and dimers has been characterized, including the presence of solvent molecules. Finally, the variation of the optical rotatory power of the cluster has been studied.

CHART 1

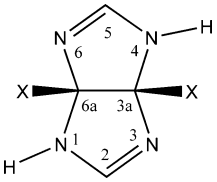

Methods

The geometry of the monomers, complexes, and proton-transfer transition-state (TS) structures has been optimized within the Gaussian 03 package[27] at the B3LYP/6-31+G** computational level.[28−30] The minimum and TS nature of the structures has been confirmed by frequency calculation at the same computational level. A further optimization has been carried

* To whom correspondence should be addressed. E-mail: ibon@iqm.csic.es. Fax: 91 564 48 53.

10.1021/jp056886g CCC: $33.50
Published on Web 01/21/2006

out in some cases at the B3LYP/6-311+G**[31] and MP2/6-311+G** levels.[32]

The interaction energy has been calculated as the difference between the total energy of the complexes and the isolated energies of the monomers. The inherent basis set superposition error, BSSE, has been taken into account using the full counterpoise method as defined by Boys and Bernardi[33] and implemented in the Gaussian 03 program.

The electron density has been analyzed using the AIM methodology[34] and the AIMPAC[35] and MORPHY programs.[36] The atomic integration has been carried out using the default parameters in the MORPHY program except for those atoms where the integrated Laplacian was larger than 1.0 10^{-3}. Ideally, the integrated Laplacian within an atomic basin should be equal to zero. However, previous studies have shown that systems, in wich all the atoms have an integrated Laplacian smaller than the mentioned value, provide small errors in the total energy and charge partitions.[37] In the present study the energetic partition of 15 systems has been carried out, being the maximum error in the total energy of 0.97 kJ/mol and the average 0.68 kJ/mol.

The optical rotatory power (ORP) of some of the complexes has been computed at the B3LYP/6-311++G(2d,2p) computational level as recommended in previous systematic works that indicate that this level is the minimum necessary for reliable results.[38−40]

Results and Discussion

Monomers. The (3a*R*,6a*R*)-1,3a,4,6a-tetrahydroimidazo[4,5-d]imidazoles **A** (*RR* hereafter) and their enantiomers (*SS*) present two additional tautomeric forms **B** and **C** (Chart 2). These form do not show chirality if the same substituent X is present in the 3a and 6a positions in the case of **B** and independently of the X substituent in the case of **C**. The optimized **A**, **B**, and **C** structures have C_2, C_s, and C_1 symmetries, respectively. The calculated relative energies (Table 1) of these structures indicate that in the gas phase only form **A** should be populated. In the rest of the article, only the complexes of this tautomer will be considered.

CHART 2[a]

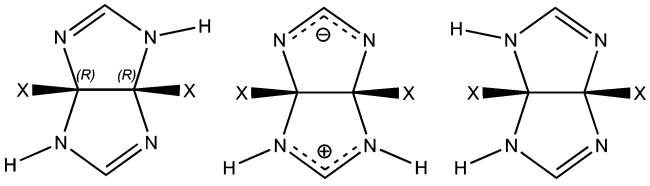

[a] The X substituent has been assumed to have the higher priority in the CIP rules to assign the configurations to stereogenic carbons.

TABLE 1: Relative Energy (kJ/mol) of the Tautomeric Forms Shown in the Scheme 2 (X = H)

Tautomer	B3LYP/6-31+G**	B3LYP/6-311+G**	MP2/6-311+G**
A	0.00	0.00	0.00
B	110.70	111.15	123.17
C	19.79	19.26	20.07

Dimers. The energies of the homo and heterochiral dimers of tetrahydroimidazo[4,5-*d*]imidazole derivatives have been gathered in Table 2. The interaction energies corrected for the BSSE are similar at the three computational levels, being almost identical in the case of the B3LYP method with the two basis set considered and about 5−10 kJ/mol larger in absolute value with respect to the MP2/6-311+G** calculations. The strongest complex corresponds to the heterochiral dimer of the fluorine derivative, and the weakest is the homochiral complex of the trifluoromethyl derivative (X = CF_3). In average, the BSSE correction amounts to 8 and 22% of the interaction energy at the B3LYP and MP2 levels, respectively.

Regarding the chiral discrimination (not corrected for the BSSE), in all the cases studied here the heterochiral complexes are more stable than the homochiral ones, ranging the differences between 3.6 kJ/mol in the dimer of the unsubtituted compound to 17.7 kJ/mol for the dimer of the CF_3 derivative. By consideration that in the dimer there are two proximal and two distal X groups, their electronic effects may need different Hammett parameters to be described. A reasonable fit is

$$\text{chiral discrimination} = -(3.7 \pm 0.2) - (10.0 \pm 0.3)(\sigma_m + \sigma_p) + (2.2 \pm 0.2)E_s$$

$$n = 7,\ r^2 = 0.997$$

which indicates that the chiral discrimination (in kJ/mol) increases when the substituent X has large and positive σ values and decreases when the substituent is voluminous (large and negative Taft's E_s values).[41]

In all the cases studied, the minimum structure for the homo and heterochiral dimers shows C_2 and C_i symmetries, respectively. Some of the geometrical parameter of these complexes have been gathered in Table 3. The N···H distances obtained at the MP2 level are shorter than those obtained at the B3LYP ones, in agreement with the larger interaction energies obtained with the former method.

With the exception of the CN group, a rough linear relationship is shown between the HB distance and the chiral discrimination ($r^2 = 0.90$). In agreement with the energetic results shown in Table 2, the heterochiral complexes exhibit shorter N···H HB distances than the corresponding homochiral ones, being the maximum difference in the CF_3 complexes where the heterochiral complex is 0.11 Å shorter than the homochiral one.

The orbital interactions, calculated with the NBO method, between the lone pair of the nitrogen atom of one monomer and the antibonding orbital of the N−H group of another have been collected in Table 4. This interaction has been shown to be responsible for the stabilization in the HB interactions. Another energy that can modulate the strength of the HB is the deformation energies, which have also been gathered in Table 4. While the orbital interactions found are attractive, the deformation energies are repulsive. In all the cases considered, the orbital interaction favored more the heterochiral complex than the homochiral one. The difference in the deformation energy is very small and slightly favors the homochiral dimer. A good linear correlation can be found between the HB distance and the orbital interaction energy ($r^2 = 0.98$) as indication that both parameters provide similar information.

The analysis of the electron density shows the presence of intermolecular bond critical points, bcp, in the HB formed and between the substituents of all the homochiral dimers, except those with the smallest substituents, X = H and F. The bcps formed due to the HB interactions show small values of the electron density (between 0.0298 and 0.0226 e) and positive values of the Laplacian (between 0.0746 and 0.0572 au). The electron density of the heterochiral dimers is always larger than that of the homochiral ones, in agreement with the shorter intermolecular distances obtained in the former complexes. Regarding the additional intermolecular bcps observed between

TABLE 2: Corrected Interaction Energy and Chiral Discrimination (kJ/mol)

		interaction energy			chiral discrimination		
X	chirality	B3LYP/6-31+G**	B3LYP/6-311+G**	MP2/6-311+G**	B3LYP/6-31+G**	B3LYP/6-311+G* *	MP2/6-311+G**
H	*RR:RR*	−46.51	−46.71	−51.64			
H	*RR:SS*	−49.89	−49.98	−54.73	−3.58	−3.35	−3.50
CH_3	*RR:RR*	−42.99	−43.11	−53.65			
CH_3	*RR:SS*	−47.21	−47.33	−58.14	−4.32	−4.40	−5.03
F	*RR:RR*	−47.31	−47.56	−51.84			
F	*RR:SS*	−56.13	−56.46	−60.13	−9.25	−9.11	−9.45
Cl	*RR:RR*	−44.77	−45.15				
Cl	*RR:SS*	−55.89	−56.13		−11.52	−11.48	
CN	*RR:RR*	−37.57	−37.98				
CN	*RR:SS*	−54.90	−55.14		−17.49	−17.42	
CCH	*RR:RR*	−43.69	−44.01				
CCH	*RR:SS*	−51.84	−52.11		−8.28	−8.37	
CF_3	*RR:RR*	−33.43	−33.33				
CF_3	*RR:SS*	−50.68	−50.99		−17.74	−18.64	

TABLE 3: Geometrical Parameters of the HB Formed in the Dimers[a]

		B3LYP/6-31+G**			B3LYP/6-311+G**			MP2/6-311+G**		
X	chirality	N−H	N···H	NHN	N−H	N···H	NHN	N−H	N···H	NHN
H	*RR:RR*	1.027	2.004	169.5	1.026	2.002	169.5	1.028	1.956	171.5
H	*RR:SS*	1.028	1.979	169.4	1.026	1.979	169.3	1.028	1.937	171.1
CH_3	*RR:RR*	1.027	2.029	171.5	1.025	2.028	171.4	1.029	1.944	172.4
CH_3	*RR:SS*	1.028	1.996	170.5	1.027	1.995	170.5	1.030	1.926	168.8
F	*RR:RR*	1.027	1.991	164.9	1.026	1.989	164.8	1.027	1.949	165.4
F	*RR:SS*	1.028	1.951	165.7	1.027	1.951	165.5	1.029	1.910	166.3
Cl	*RR:RR*	1.028	1.999	166.7	1.026	1.996	166.2			
Cl	*RR:SS*	1.093	1.944	167.3	1.208	1.942	167.0			
CN	*RR:RR*	1.028	2.009	167.7	1.026	2.009	167.2			
CN	*RR:SS*	1.029	1.958	165.8	1.027	1.960	165.0			
CCH	*RR:RR*	1.027	2.011	169.1	1.026	2.012	168.6			
CCH	*RR:SS*	1.029	1.961	169.7	1.028	1.963	169.0			
CF_3	*RR:RR*	1.026	2.075	163.4	1.025	2.072	163.3			
CF_3	*RR:SS*	1.029	1.965	172.3	1.028	1.963	171.4			

[a] Bond angles are in degrees, and bond lengths are in angstroms.

TABLE 4: Orbital Interaction Due to the HB Formation and Deformation Energy of the Monomers (kJ/mol) at the B3LYP/6-31+G Computational Level**

X	chirality	orbital interaction per HB	deformation energy per monomer
H	RR:RR	−67.91	2.10
H	RR:SS	−72.43	2.16
CH_3	RR:RR	−60.21	1.87
CH_3	RR:SS	−69.37	1.99
F	RR:RR	−69.62	2.05
F	RR:SS	−76.99	2.20
Cl	RR:RR	−67.11	1.89
Cl	RR:SS	−78.41	2.10
CN	RR:RR	−65.14	1.73
CN	RR:SS	−76.15	2.01
CCH	RR:RR	−65.19	1.64
CCH	RR:SS	−75.65	1.89
CF_3	RR:RR	−49.58	1.73
CF_3	RR:SS	−72.72	1.89

the substituents, the electron density and Laplacian corresponds to that of van der Waals interactions. Energetically, the formation of new bcps has been shown to be a source of stabilization of the atoms involved.[42] However, in many cases this stabilization is compensated by a loss of energy in the rest of the molecule[43] as happened in the homochiral complexes studied here.

By use of the possibilities of the AIM methodology to partition the total energy in atomic contributions, we have explored how the energy gain due to the dimer formation is redistributed and which are the atoms responsible for the chiral discrimination. In Table 5, the energetic variation of the atomic energies due to the complexation for some of the complexes studied is presented.

The atoms of the HB donor moiety (N1 and H1) are the ones that suffer the largest changes, which is clearly associated to the largest variation of the atomic charges (−0.07 and 0.08 for the N1 and H1 atoms in the homochiral dimer of the unsubstituted compound). The result for the HB donor moiety is an overall gain between 5 and 38 kJ/mol. The HB acceptor atom (N6) increases its energy in 40 kJ/mol in average. The energy destabilization and loss of charge of the hydrogen atom was one of the criterion defined by Koch and Popelier to characterize HBs.[44] The positive energy variation of the N4−H4 group and the negative one of the N3 atom (none of them involved in the HB formation) are significant.

The representation of the energy variation vs the charge variation (Figure 1) shows that these two parameters are related, but the relationship is more complex than a simple linear relation and presents significant deviations.

By use of the same partition, the atomic energy differences in the diastereomeric complexes (*RR:RR* vs *RR:SS*) can be compared (Table 6). The atomic energetic differences are very different for each case. All the groups that are in the side of the molecule involved in the HB formation (N1−H1, C3−X3a, and N6) favored the heterochiral complex, with the exception of the N1−H1 moiety of the fluorine derivatives, which show positive values. If the average quantities of each atom are calculated along the studied dimers, negative values for N1 and N3 (−10.5 and −11.5 kJ/mol, respectively) and positive values

TABLE 5: Variation of the Atomic Energy (kJ/mol) upon Dimerization Obtained with the AIM Methodology at the B3LYP/6-31+G Computational Level[a]**

	H(*RR:RR*)	H(*RR:SS*)	F(*RR:RR*)	F(*RR:SS*)	Cl(*RR:RR*)	Cl(*RR:SS*)	CN(*RR:RR*)	CN(*RR:SS*)	CCH(*RR:RR*)	CCH(*RR:SS*)
N1	**−164.73**	**−169.00**	**−134.29**	**−131.73**	**−115.87**	**−136.27**	**−114.64**	**−134.50**	**−132.78**	**−143.39**
H1	***128.04***	***131.32***	***116.57***	***119.64***	***110.72***	***118.06***	***102.72***	***110.86***	***116.99***	***123.67***
C2	10.00	6.75	−2.51	−6.12	−10.08	−6.72	−5.11	0.36	0.25	0.29
H2	−5.05	−2.14	−4.44	1.20	−6.24	1.98	−6.62	4.82	−5.99	0.89
N3	41.76	42.87	35.16	29.50	24.68	23.39	29.23	28.55	37.14	36.61
C3a	6.26	6.61	6.13	1.32	8.30	9.47	7.71	9.05	5.73	7.06
X3a	−2.90	−3.42	3.73	4.52	1.89	−0.92	2.06	−1.38	−1.60	−3.49
N4	−40.16	−45.06	−69.47	−64.85	−68.80	−71.04	−65.32	−61.31	−45.59	−48.49
H4	6.57	7.19	11.21	11.93	10.27	12.09	11.22	13.50	7.11	8.30
C5	22.16	21.81	36.63	33.74	30.87	33.82	30.76	31.91	24.82	27.19
H5	−1.13	1.70	−0.93	5.13	−1.60	5.57	−1.54	7.41	−1.92	3.68
N6	−41.56	−44.01	−36.85	−44.32	−35.10	−52.17	−24.09	−41.26	−35.64	−49.17
C6a	19.91	23.25	10.95	−3.74	10.13	13.77	15.98	16.28	21.50	21.72
X6a	−3.45	−3.78	3.12	14.20	15.88	18.25	−11.03	−6.99	−13.27	−12.93

[a] Because of the symmetry of the systems, only the atoms of one monomer are given. Numbering as in Scheme 1: the groups involved in the HB are the N1−H1 and N6.

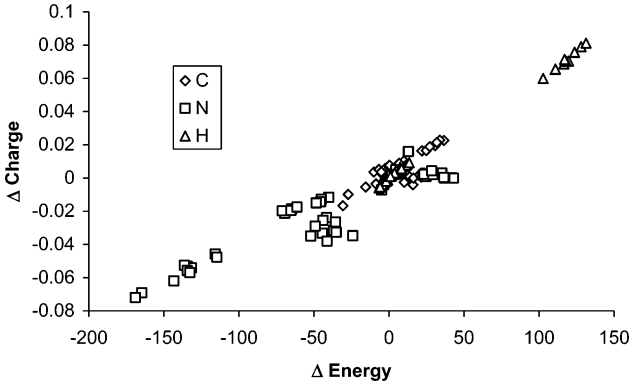

Figure 1. Atomic variation of charge and energy between the isolated monomers and the dimers.

TABLE 6: Atomic Energy Differences between the Homo- and Heterochiral Dimers (kJ/mol)[a] Obtained with the AIM Methodology at the B3LYP/6-31+G Computational Level**

	X				
atom	H	F	Cl	CN	CCH
N1	−4.27	2.56	−20.41	−19.85	−10.60
H1	3.29	3.07	7.34	8.14	6.68
C2	−3.25	−3.61	3.36	5.47	0.04
H2	2.91	5.64	8.22	11.44	6.89
N3	1.11	−5.66	−1.29	−0.68	−0.53
C3a	0.35	−4.80	1.17	1.34	1.33
X3a	−0.52	0.79	−2.81	−3.44	−1.89
N4	−4.91	4.62	−2.24	4.01	−2.90
H4	0.61	0.72	1.82	2.28	1.19
C5	−0.35	−2.89	2.95	1.15	2.38
H5	2.83	6.06	7.16	8.95	5.59
N6	−2.45	−7.47	−17.07	−17.17	−13.53
C6a	3.34	−14.69	3.64	0.29	0.22
X6a	−0.33	11.08	2.36	−11.00	0.34

[a] Negative values indicate that the corresponding atom in the heterochiral dimer is more stable than in the homochiral one.

for all the hydrogen atoms (5kJ/mol in average) are obtained. In the rest of the cases, the variations are compensated along the series.

Trimers and Larger Clusters. To understand the behavior of these compounds in the solid phase, several clusters with up to seven monomers of the parent compound have been explored. The clusters studied have been chosen in such a way that an element of symmetry (C_2 or C_i) will be present to reduce the computational cost of the calculations, with the exception of one of the trimers. The energy results are reported in Table 7. The main effect in the interaction energy corresponds to the number of monomers included in the cluster, but the distribution of the monomers within the complexes should be not rule out. Thus, a difference of 14.6 kJ/mol is observed in the hexamer with three monomers of each enantiomer that differ in their disposition (*RR:SS:RR:SS:RR:SS* and *RR:RR:RR:SS:SS:SS*).

TABLE 7: Energy Results (kJ/mol) of the Larger Clusters of the Parent Compound X = H of the Tetrahydroimidazoimidazole at the B3LYP/6-31+G Computational Level**

no. monomers	chirality	E_I	E_{chiral}
3	*RR:RR:RR*	−103.42	0.00
3	*RR:SS:RR*	−110.68	−7.27
3	*RR:RR:SS*	−107.14	−3.72
4	*RR:SS:RR:SS*	−168.80	−11.17
4	*RR:SS:SS:RR*	−164.89	−7.26
4	*RR:RR:SS:SS*	−161.48	−3.86
4	*RR:RR:RR:RR*	−157.62	0.00
5	*RR:RR:RR:RR:RR*	−212.19	0.00
5	*RR:SS:RR:SS:RR*	−227.05	−14.86
5	*RR:RR:SS:RR:RR*	−219.71	−7.52
5	*SS:RR:RR:RR:SS*	−219.90	−7.71
6	*RR:RR:RR:RR:RR: RR*	−266.09	0.00
6	*RR:SS:RR:SS:RR: SS*	−285.08	−18.99
6	*RR:RR:RR:SS:SS: SS*	−270.40	−4.30
6	*RR:SS:RR:RR:SS: RR*	−281.52	−15.42
6	*RR:SS:SS:SS:SS:R R*	−273.77	−7.68
6	*RR:RR:SS:SS:RR: RR*	−274.14	−8.04
7	*RR:RR:RR:RR:RR: RR:RR*	−320.58	0.00
7	*RR:SS:RR:SS:RR: SS:RR*	−342.94	−22.36

We have found that the interaction energy results, including those of the dimers of the parent compound, can be correlated with the number of hydrogen bonds and the adjacent homochiral interactions in each cluster (...:*RR*:*RR*:... or ...:*SS*:*SS*:...): $E_I = 5.11 - 29.05(\text{no. HB}) + 3.73(\text{no. homochiral interactions})$, $n = 21$, $r^2 = 1.0000$, SD = 0.22. This equation clearly shows that the homochiral interactions are additive and that each one destabilize the interaction energy by 3.73 kJ/mol. Since the HB can be formed and broken easily in nature, the formation of large clusters or even crystals should favor the alternate structure, which is the most stable one.

In addition to the energy differences observed within the cluster, the geometrical topology of them is clearly different. While the clusters with the alternate enantiomers show an undulating linear ribbon secondary structure, the homochiral clusters present a helical shape as shown in Figure 2.

Racemization Process. Two mechanisms can be responsible of the transformation of one enantiomer in its mirror image, the inversion of the 3a and 6a carbon atoms and the proton

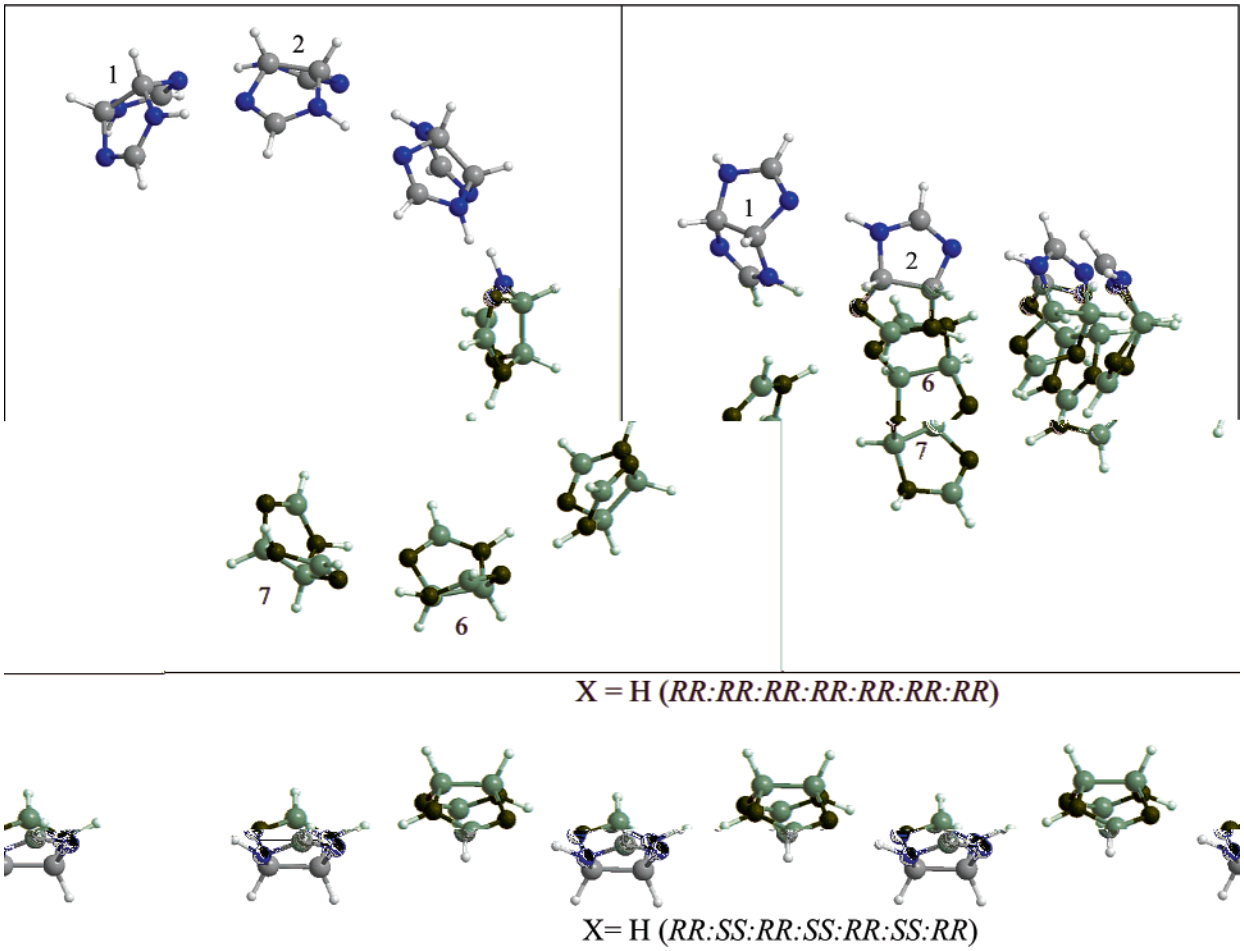

Figure 2. Optimized geometry of the homochiral heptamer cluster (two views) and the alternate one.

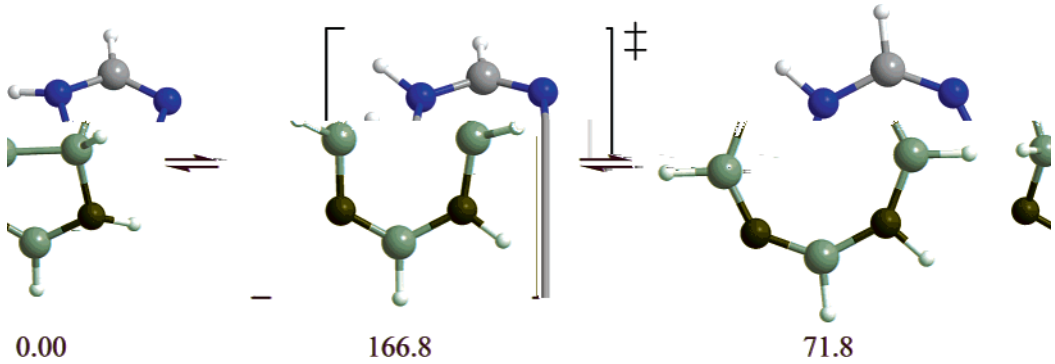

Figure 3. Racemization mechanism through carbon-inversion ring opening. The relative energies are in kJ/mol.

transfer between the two adjacent nitrogen atoms. The first mechanism, in general, is associated with a much higher energy barrier. However in this case, the system can evolve through a planar eight-membered ring as intermediate structure being the corresponding TS barrier of 166.8 kJ/mol (Figure 3). A further transformation of the planar intermediate can generate the opposite enantiomer.

The experimental oxidation of several tetrahydroimidazo−imidazole derivatives affords the corresponding tetrazocine (Scheme 1),[45,46] which is the oxidized analogue of the reaction intermediate found in Figure 3.

The other possibility for the racemization of these products corresponds to the proton transfer between nitrogen atoms of different rings. The barriers of these processes have been shown to be very dependent on the presence of additional molecules that cooperate in the mechanism. Thus the complete surface

SCHEME 1

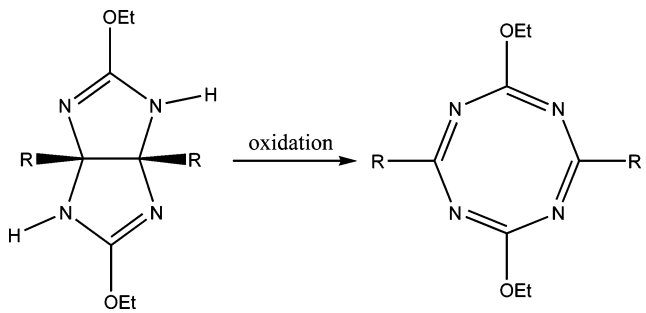

has been explored for the monomer and dimers alone and in the presence of one and two water molecules. The calculated structures and the relative energies for the monomer and its complexes with one and two water molecules are represented

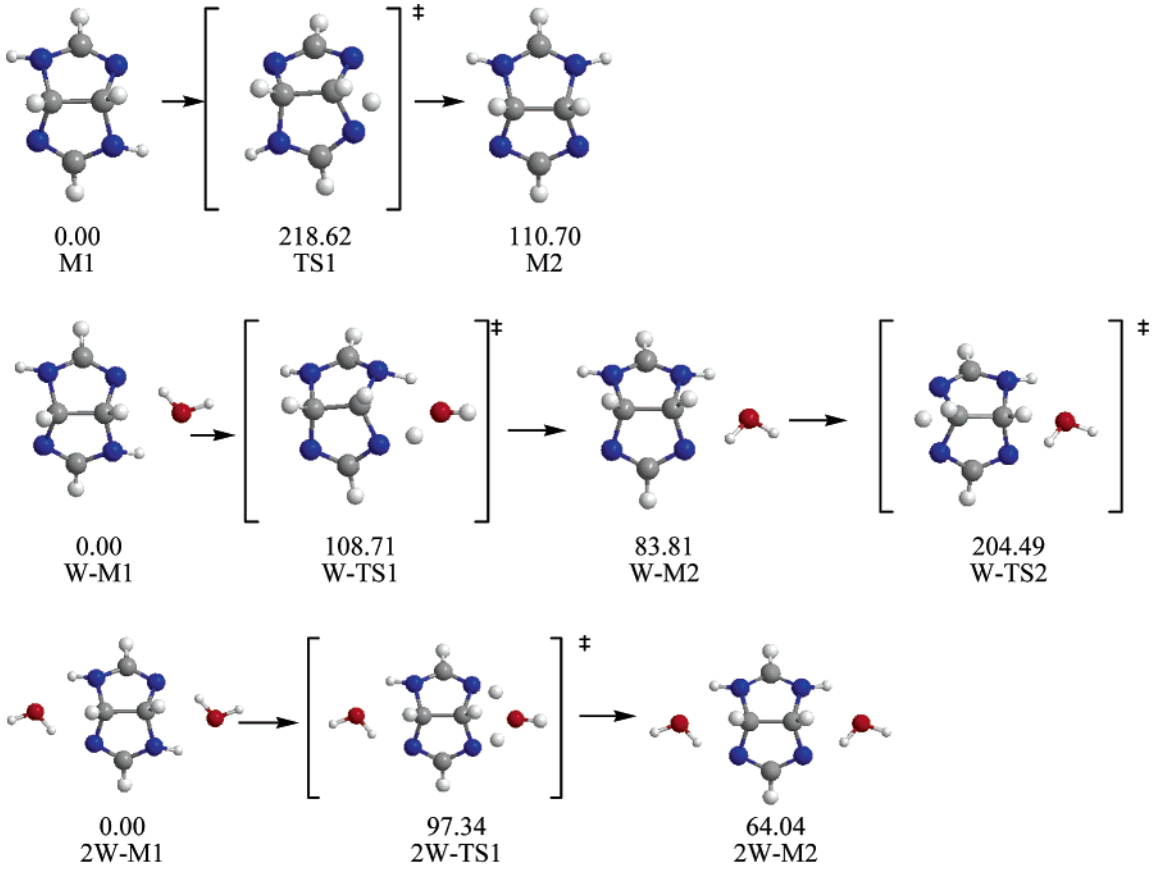

Figure 4. Minimum and TS structures involved in the proton-transfer processes of the isolated monomers and their corresponding complexes with one and two water molecules. Relative energies are in kJ/mol. Because of the symmetry of the process, only one-half of the structures are shown.

in Figure 4. The process evolved through the high-energy zwiterionic tautomer, studied previously (Chart 2B). The activation barrier for proton transfer within the isolated monomer is very high (218.6 kJ/mol) in accordance with previous studies for similar processes[9,47]

The assistance of one water molecule reduces in half the proton-transfer barrier (108.7 kJ/mol, W-TS1) and even more in the case of the presence of two water molecules (97.3 kJ/mol, 2W-TS1). The presence of water molecules stabilizes the zwiterionic intermediate (W-M2 and 2W-M2) due to the formation of strong HBs (interaction energies of −69.38 and −134.26 kJ/mol, respectively). It is significant that the presence of a water molecule in one side of the imidazoimidazole stabilizes by 14 kJ/mol the proton-transfer TS in the other side (W-TS2). Only in the case where the imidazoimidazole is solvated with two molecules of water does the limiting step in the proton-transfer process (2W-TS1) have an energy barrier smaller than the one obtained for the inversion of the carbon atoms as shown in Figure 3.

The proton-transfer surface for the heterochiral dimer has been represented in Figure 5, being similar to that of the homochiral dimer. In addition, the energy differences of the structures with respect to the most stable configuration for each case and the energy difference between the homochiral structure and the corresponding heterochiral one (Echir) have been included.

As previously shown, the proton transfer evolves through the zwiterionic tautomer. The complete reaction starts with the transfer of one of the outer protons, followed by the asynchronous double transfer of the central ones and finally the outer proton of the opposite side. An alternative mechanism corresponds to an initial double proton transfer of the inner hydrogens that will generate a dimer with two zwiterionic tautomers, but this structure is not stable and reverts toward the initial one.

The general energy profiles of the homo and heterochiral dimers are very similar. In all the cases the relative energies, with respect to the initial structure, of the TS and intermediate structures are slightly smaller in the heterochiral complex than in the homochiral one. For this reason, most of the discussion will be carried out using the energy values of the heterochiral complex but can be extrapolated with small variations to the homochiral case.

The results obtained in the case of the isolated dimer show high similarities with the ones obtained for the monomers solvated by a water molecule and, thus, the relative energy of the *RR:SS*-M2 is similar to that of W-M2 and *RR:SS*-TS2 with W-TS1 and *RR:SS*-TS1 with W-TS2 which indicates that the second imidazoimidazole molecule and the water molecule play similar roles. As in the case of the monomer, the HB between the water molecule and the zwitterionic tautomer stabilizes the corresponding complexes as can be observed when comparing *RR:SS*-WM2 and *RR:SS*-WM3, that differ in 15 kJ/mol. Another effect due to the presence of water molecules is the reduction of the inner proton-transfer barrier as shown in the comparison of the *RR:SS*-TS2 (105.14 kJ/mol), *RR:SS*-WTS2 (93.84 kJ/mol), and *RR:SS*-2WTS2 (84.19 kJ/mol).

With regard to the limiting TS, in all the cases, this corresponds to the proton transfer of one of the outer protons. However, in the dimer solvated with two water molecules, the energy differences between the TS of the inner (*RR:SS*-2WTS2) and outer hydrogens (*RR:SS*-2WTS1) range between 3.4 and 5.8 kJ/mol.

The structures and energy differences for the proton transfer in two of the trimers are shown in Figure 6. The energetic profile

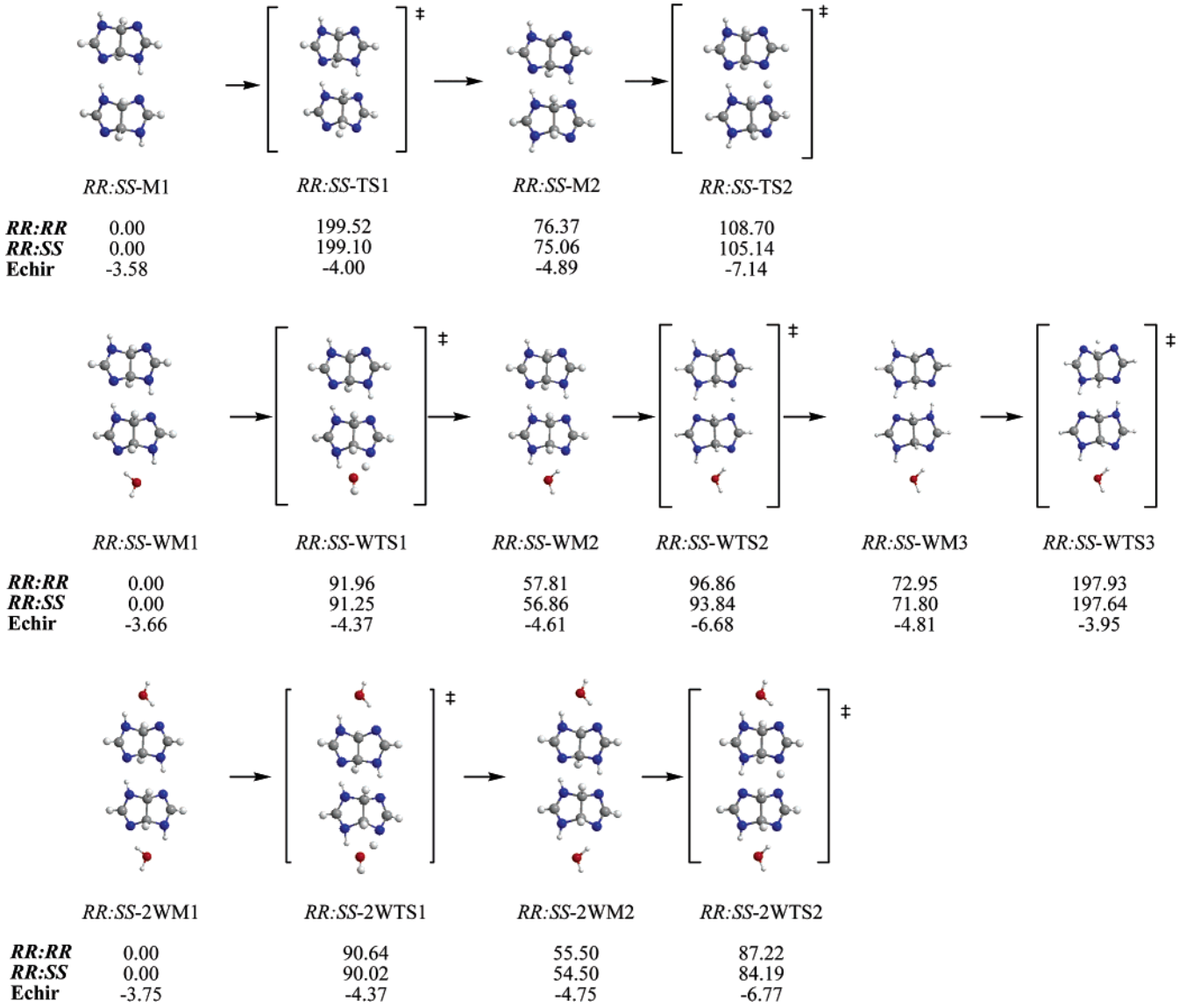

Figure 5. Minimum and TS structures involved in the proton-transfer processes of the heterochiral dimer and their corresponding complexes with one and two water molecules. The relative energies of the reaction in the homochiral and heterochiral as well as the chiral discrimination are reported (kJ/mol). Because of the symmetry of the process, only one-half of the structures are shown.

is very similar to the one obtained for the dimers. An interesting difference is observed for the stabilization due to the increment of the chain in the inner proton transfer (*RR:SS:RR*-TS2 and *RR:SS:RR*-2WTS2) when compared to the corresponding ones in the dimers. Again the limiting step corresponds to the transfer of the external proton; once this is achieved, the rest of the TS and the intermediate are below this barrier indicating that the proton will be transferred freely generating a barrierless racemization along the chain in a wavelike expansion.

The chiral discrimination energy differences increase in the intermediate structures and especially in the TS structures that correspond to the double inner proton transfer (*RR:SS*-TS2, *RR:SS*-WTS2, *RR:SS*-2WTS2, *RR:SS:RR*-TS2 and *RR:SS:RR*-2WTS2). Similar increments of the chiral discrimination have been described in other proton-transfer processes and have been associated to the contraction of the systems in the TS that increment the energetic penalty in the homochiral system.[5,9]

ORP. The calculated ORPs of some of the clusters considered in the present article are reported in Table 8. The simple dimerization process produces a change of sign and a very important variation of the magnitude of the ORP. Similar tendencies have been found for other systems, both experimentally and theoretically.[10, 48]

The influence of the arrangement of the chiral monomers within the cluster is clearly shown in the two trimers that present two monomers with *SS* and one with *RR* chirality. In the case where the *RR* monomer is in the middle, the ORP value is only 9.2 while when it is at the end of the cluster the ORP value is −115.3 kJ/mol. Something similar happens with the *RR:SS:SS:RR* tetramer when compared to the *RR:SS:RR:SS* and *RR:RR:SS:SS* tetramers, which is due to the C_i symmetry, have null ORP values.

By use of the data shown in Table 8 and that of their corresponding enantiomeric clusters, a correlation between the ORP and the number of homochiral interactions (1 for each *SS:SS* interaction, 0 for *RR:SS* or *SS:RR*, and −1 for each *RR:RR* interaction) and the number of monomers (a value of 1 is given for each *SS* monomer and −1 for the *RR* ones) has been obtained.

ORP = −(126.2 ± 3.3)(no. homochiral interactions) + (11.4 ± 2.3)(no. monomers *SS* − *RR*), $n = 17$, $r^2 = 0.998$. This equation shows that the main effect on the ORP value came

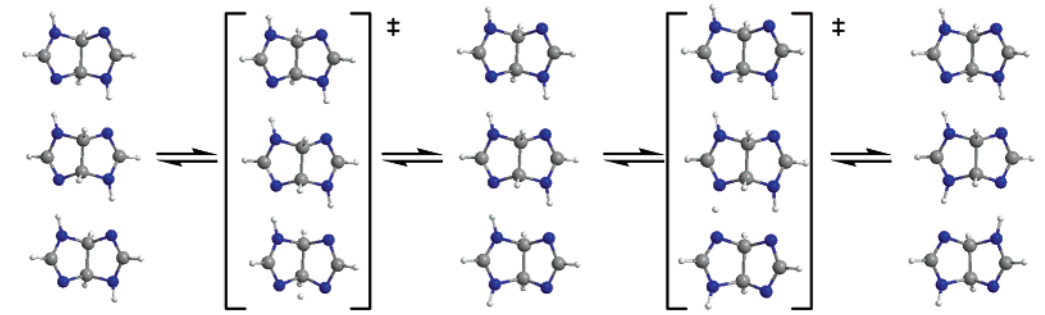

	RR:SS:RR M1	*RR:SS:RR* TS1	*RR:SS:RR* M2	*RR:SS:RR* TS2	*RR:SS:RR* M3
RR:RR:RR	0.00	197.42	72.72	94.61	52.75
RR:SS:RR	0.00	196.94	71.27	91.18	50.90
Echir	-7.27	-7.75	-8.72	-10.70	-9.11

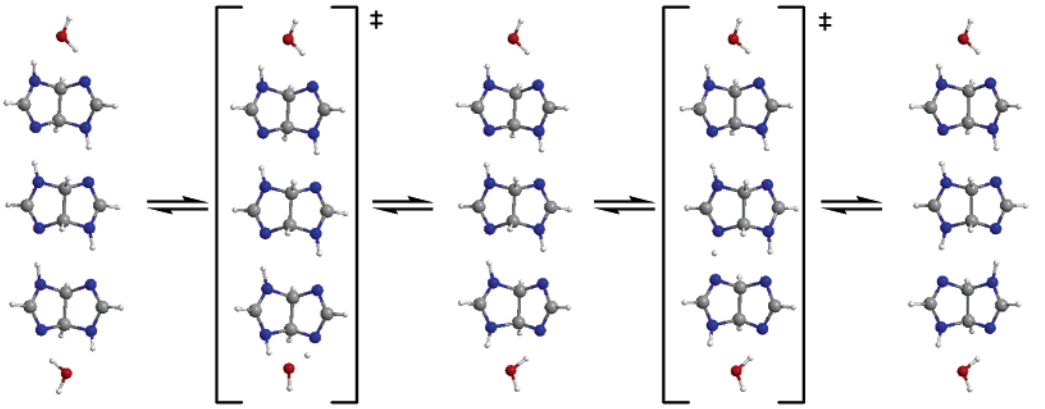

	RR:SS:RR 2WM1	*RR:SS:RR* 2WTS1	*RR:SS:RR* 2WM2	*RR:SS:RR* 2WTS2	*RR:SS:RR* 2WM3
RR:RR:RR	0.00	89.80	54.67	81.61	48.58
RR:SS:RR	0.00	89.21	53.49	76.67	46.47
Echir	-7.19	-7.78	-8.36	-12.13	-9.30

Figure 6. Minimum and TS structures involved in the proton-transfer processes of the *RR:SS:RR* trimer and their corresponding complexes with two water molecules. The relative energies of the reaction in the homochiral and heterochiral as well as the chiral discrimination are reported (kJ/mol). Because of the symmetry of the process only one-half of the structures are shown.

TABLE 8: Optical Rotatory Power (in Degrees) of Some of the Cluster Studied

no. monomers	chirality	optical rotatory power	no. *SS:SS*−*RR:RR* interactions	no. *SS*−*RR* monomers
1	*SS*	20.99	0	1
2	*SS:SS*	−116.91	1	2
2	*RR:SS*	0.00[a]	0	0
3	*SS:SS:SS*	−210.36	2	3
3	*SS:SS:RR*	−115.32	1	1
3	*SS:RR:SS*	9.20	0	1
4	*RR:SS:SS:RR*	−125.46	1	0
4	*SS:SS:SS:SS*	−333.55	3	4
4	*RR:SS:RR:SS*	0.00[a]	0	0
4	*RR:RR:SS:SS*	0.00[a]	0	0

[a] Null value of ORP due to symmetry conditions.

from the homochiral interactions with a small correction due to the effect of the monomers.

Conclusions

A theoretical study of the chiral discrimination of different tetrahydroimidazo[4,5-*d*]imidazole derivatives dimers has been carried out using DFT methods (B3LYP/6-31+G** and B3LYP/6-311+G**). The results show that in all the cases the heterochiral dimer (*RR:SS* or *SS:RR*) is more stable than the homochiral one (*RR:RR* or *SS:SS*) up to 17.5 kJ/mol for the cases studied. The distance in the hydrogen bonds, orbital interactions, and electron density at the bcps are in agreement

with the favored stability of the heterochiral dimer. The atomic partition of the electron density using the AIM methodology shows that the atoms in the HB donor moiety are the ones that more vary their energy when compared to the monomers. The energetic gain due to the dimer formation is redistributed in the whole system in a nonuniform way, stabilizing the two nitrogen atoms involved in the HB, and destabilizing the hydrogen atom of the HB.

The atomic contribution to the chiral discrimination shows that the moieties in the face where the HB occur favored the heterochiral complex while the hydrogen atoms are more stable in the homochiral complex.

Clusters up to heptamers have been studied in order to understand the possible behavior of these systems in the formation of fibers or crystalline structures. The alternate disposition of the monomers of different chirality within the cluster is favored. The interaction energy has been correlated with the number of HBs and the number of homochiral interactions. In addition, the geometrical topology of the homochiral clusters tends to form helixes while the alternated clusters show an undulating linear ribbon shape.

Two mechanisms of transformation of one of the enantiomers into the mirror image one have been explored. The first one consists of the inversion of the carbon atoms evolving through a planar eight-membered ring into the other enantiomer. The second one corresponds to the simultaneous transfer of the two protons attached to the nitrogen of these molecules. In this case, the monomer and the two dimers have been studied, isolated, and in the presence of one and two water molecules. The involvement of an additional molecule, water or another imadazoimidazole, reduces significantly the proton-transfer barrier. The chiral discrimination in the TS and intermediates studied for the dimers is larger than in the most stable dimer due to the higher energy values of the homochiral derivatives when compared to the heterochiral ones.

Finally, the optical rotatory power of some of the derivatives has been computed. A small value has been obtained for the isolated monomer, but the formation of clusters increases significantly the values obtained. The ORP values have been correlated with the number of homochiral interactions and the number of monomers of each enantiomeric form within the cluster.

Acknowledgment. This work was carried out with financial support from the Ministerio de Ciencia y Tecnología (Project No. BQU-2003-01251). Thanks are given to the CTI (CSIC) and CESGA for allocation of computer time.

Supporting Information Available: Hammet and E_s parameters of the substituents used in this article. Coordinates of all the structures calculated at the B3LYP/6-31+G** computational level. This material is available free of charge via the Internet at http://pubs.acs.org

References and Notes

(1) Craig, D. P., Chiral discrimination. In *Optical activity and chiral discrimination*; Mason, S. F., Ed.; Reidel Publising Company: 1978; pp 293−318.

(2) Tobe, Y. *Mendeleev Commun.* **2003**, 93−94.

(3) Alkorta, I.; Elguero, J. *J. Am. Chem. Soc.* **2002**, *124*, 1488−1493.

(4) Alkorta, I.; Elguero, J. *J. Chem. Phys.* **2002**, *117*, 6463−6468.

(5) Picazo, O.; Alkorta, I.; Elguero, J. *J. Org. Chem.* **2003**, *68*, 7485−7489.

(6) Alkorta, I.; Elguero, J. *THEOCHEM* **2004**, *680*, 191−198.

(7) Liu, S. Z.; Zhou, Z. Y.; Gong, X. L.; Donga, X. L. *THEOCHEM* **2005**, *717*, 121−125.

(8) Picazo, O.; Alkorta, L.; Eiguero, J.; Mo, O.; Yanez, M. *J. Phys. Org. Chem.* **2005**, *18*, 491−497.

(9) Picazo, O.; Alkorta, I.; Elguero, J. *Struct. Chem.* **2005**, *16*, 339−345.

(10) Alkorta, I.; Picazo, O.; Elguero, J. *J. Phys. Chem. A* **2005**, *109*, 3262−3266.

(11) Alkorta, I.; Picazo, O.; Elguero, J. *Tetrahedron: Asymmetry* **2004**, *15*, 1391−1399.

(12) Du, D. M.; Fu, A. P.; Zhou, Z. Y. *Chem. Phys. Lett.* **2004**, *392*, 162−167.

(13) Du, D. M.; Fu, A. P.; Zhou, Z. Y. *Int. J. Quantum. Chem.* **2005**, *101*, 340−347.

(14) Portmann, S.; Inauen, A.; Luthi, H. P.; Leutwyler, S. *J. Chem. Phys.* **2000**, *113*, 9577−9585.

(15) Dong, X. L.; Zhou, Z. Y.; Liu, S. Z.; Gong, X. L. *THEOCHEM* **2005**, *718*, 9−15.

(16) Al-Rabaa, A.; LeBarbu, K.; Lahmani, F.; Zehnacker-Rentien, A. *J. Phys. Chem. A* **1997**, *101*, 3273−3278.

(17) Speranza, M. *Adv. Phys. Org. Chem.* **2004**, *39*, 147−281.

(18) King, A. K.; Howard, B. J. *Chem. Phys. Lett.* **2001**, *348*, 343−349.

(19) Borho, N.; Haber, T.; Suhm, M. A. *Phys. Chem. Chem. Phys.* **2001**, *3*, 1945−1948.

(20) Borho, N.; Suhm, M. A. *Org. Biomol. Chem.* **2003**, *1*, 4351−4358.

(21) Beu, T. A.; Buck, U. *Z. Phys. Chem.* **2000**, *214*, 437−447.

(22) Le Barbu, K.; Brenner, V.; Millie, P.; Lahmani, F.; Zehnacker-Rentien, A. *J. Phys. Chem. A* **1998**, *102*, 128−137.

(23) Le Barbu, K.; Lahmani, F.; Zehnacker-Rentien, A. *J. Phys. Chem. A* **2002**, *106*, 6271−6278.

(24) Guidoni, A. G.; Piccirillo, S.; Scuderi, D.; Satta, M.; Di Palma, T. M.; Speranza, M. *Phys. Chem. Chem. Phys.* **2000**, *2*, 4139−4142.

(25) Latini, A.; Satta, M.; Guidoni, A. G.; Piccirillo, S.; Speranza, M. *Chem.−Eur. J.* **2000**, *6*, 1042−1049.

(26) Paladini, A.; Calcagni, C.; Di Palma, T.; Speranza, M.; Lagana, A.; Fago, G.; Filippi, A.; Satta, M.; Guidoni, A. G. *Chirality* **2001**, *13*, 707−711.

(27) Frisch, M. J.; Trucks, G. W.; Schlegel, H. B.; Scuseria, G. E.; Robb, M. A.; Cheeseman, J. R.; Montgomery, J. A., Jr.; Vreven, T.; Kudin, K. N.; Burant, J. C.; Millam, J. M.; Iyengar, S. S.; Tomasi, J.; Barone, V.; Mennucci, B.; Cossi, M.; Scalmani, G.; Rega, N.; Petersson, G. A.; Nakatsuji, H.; Hada, M.; Ehara, M.; Toyota, K.; Fukuda, R.; Hasegawa, J.; Ishida, M.; Nakajima, T.; Honda, Y.; Kitao, O.; Nakai, H.; Klene, M.; Li, X.; Knox, J. E.; Hratchian, H. P.; Cross, J. B.; Adamo, C.; Jaramillo, J.; Gomperts, R.; Stratmann, R. E.; Yazyev, O.; Austin, A. J.; Cammi, R.; Pomelli, C.; Ochterski, J. W.; Ayala, P. Y.; Morokuma, K.; Voth, G. A.; Salvador, P.; Dannenberg, J. J.; Zakrzewski, V. G.; Dapprich, S.; Daniels, A. D.; Strain, M. C.; Farkas, O.; Malick, D. K.; Rabuck, A. D.; Raghavachari, K.; Foresman, J. B.; Ortiz, J. V.; Cui, Q.; Baboul, A. G.; Clifford, S.; Cioslowski, J.; Stefanov, B. B.; Liu, G.; Liashenko, A.; Piskorz, P.; Komaromi, I.; Martin, R. L.; Fox, D. J.; Keith, T.; Al-Laham, M. A.; Peng, C. Y.; Nanayakkara, A.; Challacombe, M.; Gill, P. M. W.; Johnson, B.; Chen, W.; Wong, M. W.; Gonzalez, C.; Pople, J. A. *Gaussian 03*; Gaussian, Inc., Pittsburgh, PA, 2003.

(28) Becke, A. D. *J. Chem. Phys.* **1993**, *98*, 5648−5652.

(29) Lee, C. T.; Yang, W. T.; Parr, R. G. *Phys. Rev. B* **1988**, *37*, 785−789.

(30) Harihara, Pc; Pople, J. A. *Theor. Chim. Acta* **1973**, *28*, 213−222.

(31) Frisch, M. J.; Pople, J. A.; Binkley, J. S. *J. Chem. Phys.* **1984**, *80*, 3265−3269.

(32) Møller, C.; Plesset, M. S. *Phys. Rev.* **1934**, *46*, 618−622.

(33) Boys, S. F.; Bernardi, F. *Mol. Phys.* **1970**, *19*, 553.

(34) Bader, R. F. W. *Atoms in Molecules: A Quantum Theory*; Clarendon Press: Oxford, 1990.

(35) Bieglerkonig, F. W.; Bader, R. F. W.; Tang, T. H. *J. Comput. Chem.* **1982**, *3*, 317−328.

(36) Popelier, P. L. A. *MORPHY98, a topological analysis program*, 0.2; 1999.

(37) Alkorta, I.; Picazo, O. *Arkivoc* **2005**, *ix*, 305−320.

(38) Cheeseman, J. R.; Frisch, M. J.; Devlin, F. J.; Stephens, P. J. *J. Phys. Chem. A* **2000**, *104*, 1039−1046.

(39) Stephens, P. J.; Devlin, F. J.; Cheeseman, J. R.; Frisch, M. J. *J. Phys. Chem. A* **2001**, *105*, 5356−5371.

(40) Ruud, K.; Stephens, P. J.; Devlin, F. J.; Taylor, P. R.; Cheeseman, J. R.; Frisch, M. J. *Chem. Phys. Lett.* **2003**, *373*, 606−614.

(41) Hansch, C.; Leo, A.; Hoekman, D. *Exploring QSAR*; American Chemical Society: Washington, DC, 1995.

(42) Matta, C. F.; Hernandez-Trujillo, J.; Tang, T. H.; Bader, R. F. W. *Chem.−Eur. J.* **2003**, *9*, 1940−1951.

(43) Matta, C. F.; Castillo, N.; Boyd, R. J. *J. Phys. Chem. A* **2005**, *109*, 3669−3681.

(44) Koch, U.; Popelier, P. L. A. *J. Phys. Chem.* **1995**, *99*, 9747−9754.

(45) Gompper, R.; Noth, H.; Rattay, W.; Schwarzensteiner, M. L.; Spes, P.; Wagner, H. U. *Angew. Chem., Int. Ed.* **1987**, *26*, 1039−1041.
(46) Gompper, R.; Schwarzensteiner, M. L. *Angew. Chem., Int. Ed.* **1983**, *22*, 543−544.
(47) Alkorta, I.; Elguero, J. *J. Chem. Soc., Perkin 2* **1998**, 2497−2503.
(48) Goldsmith, M. R.; Jayasuriya, N.; Beratan, D. N.; Wipf, P. *J. Am. Chem. Soc.* **2003**, *125*, 15696−15697.